

Device Technologies for Photonic Networks

*Hiroshi Yasaka[†], Masayuki Okuno,
and Hirohiko Sugahara*

Abstract

High-speed and more functional optical and electrical devices are essential in constructing large-capacity and highly functional photonic networks. Here, we introduce technologies for optical signal control photonic devices and very high-speed electrical signal processing integrated circuits.

1. Introduction

Higher throughput and more functional photonic networks are required to keep up with the explosive increase in the growth of Internet communications traffic. Wavelength division multiplexing (WDM) technology is one of the best ways of increasing the throughput of photonic networks. It transmits several optical signals in a single optical fiber and the total throughput can reach up to several tera bits per second. Optical cross-connects (OXC) and optical add/drop multiplexers (OADMs) also can improve network functionality. Wavelength tunable semiconductor lasers, optical filters and switches, and ultra-high-speed signal processing integrated circuits (ICs) are essential in achieving such high-throughput and highly functional photonic networks. Here, we discuss recent research by our laboratories on optical signal control photonic devices and very high-speed electrical signal processing ICs for the next generation of photonic networks.

2. Wavelength tunable light sources

2.1 Overview of wavelength tunable semiconductor lasers

In WDM systems, the signal wavelength is used as a label and the signal is processed in accordance with

this wavelength. Network functions can be improved by applying OXCs and OADMs and by switching the optical path and signal's destination dynamically. High-speed wavelength switching is the key technology for achieving highly functional photonic network systems. Wavelength tunable semiconductor lasers are critical components for constructing next-generation highly functional photonic networks, because they cover the whole wavelength range used by the systems. They are also useful as backup light sources. In WDM systems, a large number of single-mode lasers are used as signal light sources. For full redundancy, we should prepare the same number of backup light sources in case any signal light sources fail. The number of backup light sources required in the systems can be reduced by using wavelength tunable lasers, and system costs can also be reduced, because these lasers can emit a wide range of signal channel wavelengths and can replace many signal light sources.

The lasing wavelength of a semiconductor laser can be controlled by changing the refractive index of the lasing wavelength control section in the laser cavity. This can be achieved by changing either its temperature or the amount of electric current injected into the section. Figure 1 shows the wavelength tuning range and wavelength switching speed of various kinds of wavelength tunable semiconductor lasers. Temperature-controlled wavelength tunable semiconductor lasers, temperature-controlled distributed feedback (DFB) laser diodes (LDs) and temperature-controlled DFB-LD arrays are located on the right. Their switch-

[†] NTT Photonics Laboratories
Atsugi-shi, 243-0198 Japan
E-mail: yasaka@aecl.ntt.co.jp

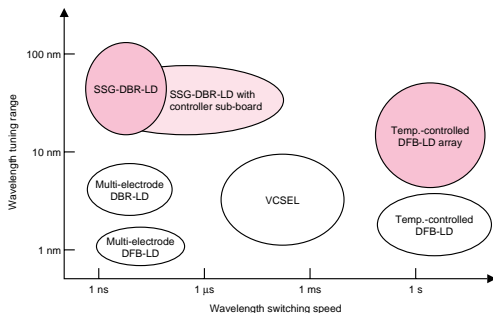


Fig. 1. Wavelength tuning range and wavelength switching speed of wavelength tunable semiconductor lasers.

ing speed is not very fast: it is several seconds. These types of lasers are applicable where the switching speed need not be very fast but the signal wavelength should be controlled stably and precisely. One example is a backup light source. On the other hand, multi-electrode DFB-LDs, multi-electrode distributed Bragg reflector (DBR) LDs, and super structure grating (SSG) DBR-LDs, located on the left of the figure, are injection-current-controlled wavelength tunable lasers. Their wavelength switching speed, which is mainly determined by the carrier lifetime in the laser's lasing wavelength control section, is around a few nanoseconds. These lasers are used for applications where the lasing wavelength needs to be switched rapidly and dynamically.

2.2 Temperature-controlled wavelength tunable semiconductor lasers

Wavelength-selectable arrayed DFB lasers have been developed [1] in our laboratories. Their lasing wavelength can be changed over a wide wavelength range by switching the DFB laser and controlling its temperature. The lasing wavelength of a conventional single DFB-LD changes by $0.1 \text{ nm}/^\circ\text{C}$. Therefore, a wavelength tuning range of more than 3 nm can be obtained with single DFB-LDs when their temperature is increased by 30°C . By fabricating a DFB-LD array in which the lasing wavelengths of the LDs are arranged in sequence at 3-nm intervals, we get a device whose output light wavelength can be changed over a wide wavelength range by switching the LD

being operated in the array and changing its temperature. Figure 2 shows a photograph of the wavelength-selectable arrayed DFB laser chip fabricated. The outputs from the 16-channel DFB-LD array are led to the monolithically integrated 16×1 multi-mode interference (MMI) coupler and semiconductor optical amplifier (SOA) through optical waveguides. The interval between the LD lasing wavelengths is 3 nm . The monolithically integrated device chip is $0.75 \times 2.35 \text{ mm}$. The chip is assembled in a butterfly module that is 27 mm long \times 16 mm wide \times 9 mm high. The size of the module is almost the same as that of a single DFB-LD. Figure 3 shows the dependence of lasing wavelength of the wavelength-selectable arrayed DFB lasers module on chip temperature. The change in lasing wavelength of each LD is about 3 nm when

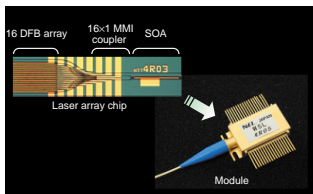


Fig. 2. Photograph of wavelength-selectable arrayed DFB laser chip and its butterfly module

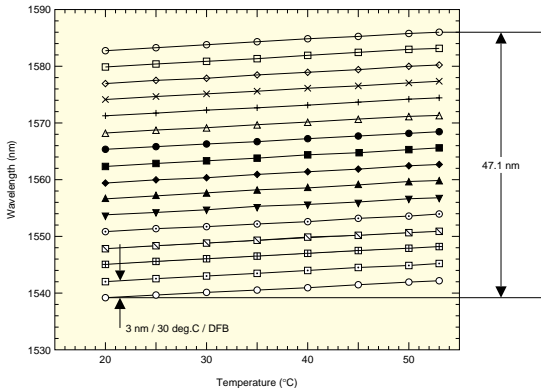


Fig. 3. Dependence of lasing wavelength of wavelength-selectable arrayed DFB laser on chip temperature.

the LD temperature increases from 20 to 53°C. The output light wavelength can be switched by selecting the LD being operated in the array. The total lasing wavelength tunable range is 47 nm. The switching speed of wavelength-selectable arrayed DFB lasers is several seconds and they are applicable as backup light sources.

2.3 Injection-current-controlled wavelength tunable semiconductor lasers

Faster wavelength tunable lasers are required in some applications. The laser's refractive index, which determines the lasing wavelength, can be changed by controlling the amount of current injected into the laser cavity or the laser's wavelength control section. The refractive index in the laser cavity can be controlled very rapidly by controlling the current injected into the laser. The wavelength switching speed is a few nanoseconds. However, the refractive index change is considerably smaller than that obtainable with the temperature control scheme. Multi-electrode DFB-LDs [2] and multi-electrode DBR-LDs [3],[4] are examples of the injection-current-controlled wavelength tunable semiconductor lasers. Multi-electrode DFB-LDs have separate current injection electrodes along with the laser cavity. The lasing

wavelength of the laser is controlled by changing the injection current distribution in the laser cavity. The tuning wavelength range is around 1 nm. The lasing wavelength in multi-electrode DBR-LDs is controlled by DBR mirrors fabricated at both sides of the laser active section. The high-reflectivity wavelength of the DBR mirror, which affects the lasing wavelength, is determined by the pitch of the corrugation grating and refractive index of the DBR section. The lasing wavelength can be changed by controlling the refractive index of the DBR section by controlling the amount of injected current. The change in refractive index in the DBR mirror is several percent, and the tuning wavelength range is around 6–7 nm.

We fabricated superstructure grating (SSG) DBR-LDs in our laboratories [5] to expand the tuning wavelength range. Unlike the conventional DBR-LDs, they have a mechanism that magnifies the tuning wavelength range. They have SSG DBR mirrors at both (front and rear) sides of the active region. These mirrors have several high-reflectivity peak wavelengths. We designed their wavelength interval to be wider in the front SSG DBR mirror than in the rear one. When the control current was injected into the rear SSG DBR mirror, the high-reflectivity peak wavelength in this section shifted towards a shorter

wavelength due to the change in refractive index. The wavelength where both SSG DBR mirrors had the same high-reflectivity peak jumped to the next shortest high-reflectivity peak wavelength of the front SSG DBR mirror. That is, the small change in the high-reflectivity peak wavelength of an SSG DBR is magnified to a value that coincides with the wavelength interval of high-reflectivity peak wavelengths. The lasing wavelength shifts toward the longer side when control current is injected into the front SSG DBR mirror. Fine tuning of the lasing wavelength can be achieved by changing the control currents to both SSG DBR mirrors simultaneously, or by changing the control current to the phase control section. The SSG-DBR-LDs demonstrated a wavelength tuning range of more than 100 nm (the maximum quasi-continuous tuning range was more than 40 nm).

Compact sub-boards of SSG-DBR-LDs with control electrical circuits have also been developed in our laboratories so that lasers can easily be used in actual network systems. In this trial, SSG-DBR-LDs integrated with SOAs were used to control the output power, independently of the change in lasing wavelength. Figure 4 shows a photograph of the SSG-DBR laser module mounted on the controller sub-board. The sub-board is 75 mm long \times 75 mm wide \times 13 mm high. The board was designed to operate with a single voltage source of +5 V. The wavelength was controlled by an electrical signal through a serial control scheme (RS-232C). The board has a memory that stores the lasing wavelength dependence on control currents injected into the active section, front and rear SSG DBR sections, and phase control section. The

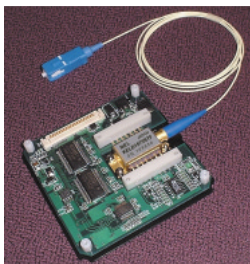


Fig. 4. Photograph of SSG-DBR laser module mounted on controller sub-board.

board could output the desired wavelength signal light when the output wavelength channel on the ITU-T standardized grids was set by sending a control electrical signal to the board through the RS-232C interface. The dependence of output power of the board on the output signal wavelength is shown in Fig. 5. The output power of a conventional device without an SOA changes in accordance with the changes in the output light wavelength. However, the output power of the board can be set at a constant value of 10 dBm, when an SSG-DBR-LD module with an integrated SOA is mounted on it. The wavelength tunable laser sub-board can emit 50 channels of wavelength signals that are adjusted to match ITU-T wavelength grids with 100-GHz intervals. The tunable wavelength range of this light source is from 1527 to 1567 nm. The wavelength switching time is less than 500 μ s, which indicates that high-speed wavelength switching can be done with the light source. Generally speaking, DBR-LDs have mode hopping problems. Theoretically, they achieve a wide wavelength tuning range by hopping the lasing mode in laser diodes. Consequently, lasing mode hopping to unexpected wavelengths might occur unexpectedly when the refractive index of the laser cavity changes as a result of degradation over an extended period of time. The wavelength tunable laser sub-board discussed above has a monitor and feedback circuits which monitor the mode stability of the laser and control its lasing mode to stabilize it automatically. That is, the wavelength tunable laser sub-board can stably emit the desired wavelength channel without any danger of unexpected mode hopping.

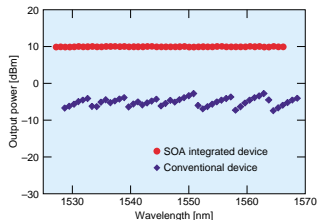


Fig. 5. Dependence of output optical power of SSG-DBR laser module mounted on controller sub-board on wavelength.

3. Silica-based planar lightwave circuit (PLC)

3.1 Overview of PLC

The silica-based planar lightwave circuit (PLC) is an optical integrated circuit with the same structure as optical fiber. PLCs are fabricated using a combination of flame hydrolysis deposition (FHD), optical fiber fabrication techniques, and reactive ion etching (RIE), which is used for fabricating LSIs [6]. PLCs are highly stable and reliable because they have no moving parts, and the waveguide material, silica glass, is physically and chemically stable. Moreover, PLCs are suitable for large-scale integration and mass production. PLCs offer easy fiber attachment and a low propagation loss of less than 0.01 dB/cm at a wavelength of 1.55 μm .

We used four types of PLC waveguide, each with a different relative refractive index difference Δ between their core and cladding. The minimum bending radius R of a waveguide and the optical fiber coupling loss depend strongly on waveguide Δ , and we selected the most suitable waveguide for the circuit type and scale. In general, a low- Δ waveguide (Δ : 0.25%, R : 25 mm) and a medium- Δ waveguide (Δ : 0.45%, R : 10 mm) are used for small-scale circuits and a high- Δ waveguide (Δ : 0.75%, R : 5 mm) is used for large-scale circuits. Recently, we have been developing a super high- Δ waveguide (Δ : 1.5%, R : 2 mm) to achieve a greater degree of integration.

Many types of circuits, including arrayed waveguide grating (AWG) multi/demultiplexers, PLC switches, interleave filters, and chromatic dispersion

compensators with a lattice-form configuration, have been developed through sophisticated design and fabrication techniques [7]. This section discusses the main PLC devices, i.e., PLC switches and AWG multi/demultiplexers.

3.2 Silica-based PLC switches

Space division optical switches are key devices in the construction of flexible and low-cost photonic networks. A PLC switch is made by combining a balanced bridge Mach-Zehnder interferometer (MZI) and the thermo-optic (TO) effect [8]. Figure 6 shows the basic configuration of a PLC switch, which is composed of two 3-dB directional couplers and two waveguide arms. These arms are equipped with thin film heaters that act as TO phase shifters. The optical path length difference ΔnL between the two arms is designed to be zero (symmetric-MZI) or a half-wavelength (asymmetric-MZI). The MZI is in the cross state when ΔnL is zero, and in the bar state when ΔnL is a half-wavelength. By varying the refractive index of one waveguide arm of the MZI using the TO effect, we can change ΔnL by half a wavelength, which changes the switch state. Typical temperature increases at the core and the heater are 15 and 40°C, respectively. The switching power is 0.35 to 0.45 W. The switching time is 1 to 3 ms, which is sufficient for OXC and OADM systems.

Large-scale switches are constructed by integrating basic switch units. One such device is the $N \times N$ strictly nonblocking matrix switch. We have already developed $N \times N$ matrix switches with a scale of up to

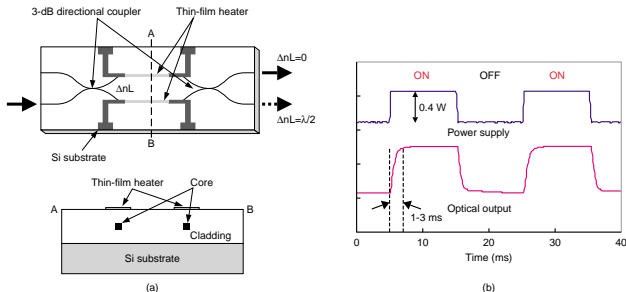


Fig. 6. Silica-based PLC switch: (a) basic structure and (b) switching response.

Table 1. Performance of fabricated PLC switches.

	N×N matrix			1×N (tree)			1×N (tap)
	4×4	8×8	16×16	1×8	1×32	1×128	1×8
Chip size (mm)	25×65	68×68	100×100	18×60	67×74	60×66	35×74
Waveguide length (cm)	14	29	66	6	13	11	17
Insertion loss (dB)	2.6	5.1	5.6	1.2	1.5	2.6	1.3
Extinction ratio (dB)	55	60	59	52	55	63	56
Power consumption (W)	3	6	13	1.5	2.2	3.5	0.5*

* Switch unit: Low power consumption type

16×16, which consist of cross-point switching units with two asymmetric MZI units. These switches allow us to obtain a high extinction ratio. Table 1 shows the performance of our fabricated matrix switches. Each switch has a low insertion loss and a high extinction ratio, which are the same features as found in mechanical switches. In particular, we realized an average insertion loss of 5.6 dB and an average extinction ratio of 59 dB in the largest 16×16 switch module. The power consumption was 13 W, which is an acceptable value for air cooling.

We have also developed 1×N switches that have 1 input port and N output ports. We used two logical arrangements for the 1×N switches. The first had a binary tree structure and the other had a tap arrangement. We arranged the gate switches at every output port to reduce crosstalk. We produced 1×8 to 1×128 switches and Table 1 lists their performance characteristics. We obtained a low insertion loss of 2.6 dB even in the 1×128 tree-type switch and a high average extinction ratio of above 50 dB.

Reducing the switching power of MZI units is a very important issue as regards the larger-scale PLC switches, and we recently developed a low power consumption technique where the switching power (45 mW) is one-tenth that of a conventional switch [9]. Many switches have been developed, including a multi-arrayed 2×2 switch for OADM systems, an OADM circuit that consists of monolithically integrated AWGs and 2×2 switches, and a low power consumption switch that uses a silicon resin.

3.3 Arrayed-waveguide grating (AWG) multi/demultiplexer

AWGs are optical filters that can simultaneously multi/demultiplex a large number of wavelength signals, and they are the *de facto* standard for WDM filters throughout the world. The AWG configuration is shown in Fig. 7. An AWG consists of input and output waveguides, two focusing slab waveguides, and arrayed-waveguides with a constant path length dif-

ference ΔL between neighboring waveguides. A thin polyimide half waveplate is inserted at the center of the arrayed-waveguides to eliminate polarization dependence due to stress-induced birefringence. The input signal light is radiated into the first slab and then coupled with the arrayed waveguides. After traveling through these waveguides, the light beams constructively interfere at one focal point in the second slab. The location of this focal point depends on the signal wavelength since the relative phase delay in each waveguide is given by $\Delta L/\lambda$. The diffractive angle is given by

$$n_s d \sin \theta + n_c \Delta L = m \lambda. \quad (1)$$

And the dispersion of focal position $dx/d\lambda$ is expressed by

$$\frac{dx}{d\lambda} = \frac{f \cdot m}{n_s \cdot d} \cdot \frac{n_g}{n_c} \quad \text{and} \quad (2)$$

$$m = \frac{n_c \cdot \Delta L}{\lambda_0}, \quad (3)$$

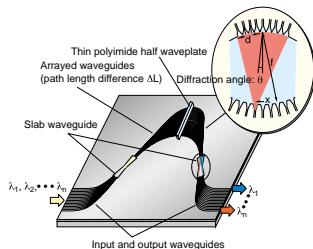


Fig. 7. Configuration of arrayed-waveguide grating (AWG).

where n_s and n_c are the respective effective indexes in the slab waveguide and channel waveguide, n_g is the group index in the channel waveguide, d is the arrayed waveguide pitch, f is the focal length of the slab waveguide, m is the diffraction order, and λ_0 is the center wavelength. By designing the ΔL value, it is possible to make AWGs with the required channel spacing and number of channels.

Figure 8 shows the progress in AWG development at NTT, which has led to the expansion in the scale of WDM system. The developed AWGs have a channel spacing of 0.2 nm (25 GHz) to 15 nm. A large-scale AWG with 400 channels was recently fabricated on one chip, and a 10-GHz-spaced 1010-channel WDM

filter that covers both the C and L fiber amplifier bands was constructed by connecting ten AWGs with a 10-GHz spacing in tandem with a primary 1-THz-spacing AWG [10]. Figure 9 is a photograph of a 25-GHz-spaced 400-channel AWG chip and its transmission spectra. The chip was fabricated using 1.5%- Δ waveguides. We obtained low losses of 3.8 to 6.4 dB and low adjacent channel crosstalk of below -20 dB over the entire C- and L-band wavelength range.

The center wavelengths for each channel in a conventional AWG depend on the temperature due to the TO effect of the silica-based waveguide. We developed an athermal AWG by filling the grooves formed at the arrayed waveguides with a silicon resin with a negative refractive index temperature dependence that cancels out the positive dependence of the silica-based waveguides [11]. An AWG has several input and output ports, and its demultiplexing characteristics depend on the input channel port number. It can achieve $N \times N$ signal interconnection when its free-spectral range (FSR) is N times the channel spacing. AWGs are also expected to be applied to an $N \times N$ full-mesh WDM system that is independent of signal bit rates and signal formats [12]. For example, a system that transmits 10-Gbit/s 32-channel signals with a throughput of 10 Tbit/s has been achieved with a full-mesh network system consisting of 32 nodes.

The AWG is a core device in photonic networks based on WDM technologies and is made by simply using silica-based PLCs, because these offer the

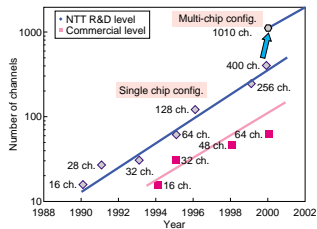
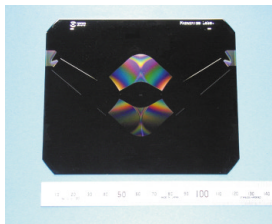
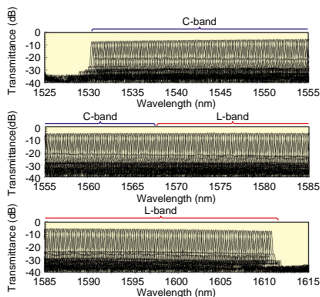


Fig. 8. AWG development.



(a)



(b)

Fig. 9. 25-GHz-spaced 400-channel AWG: (a) photograph of AWG chip and (b) transmission spectra.

advantages of low-loss and high process precision.

4. Very-high-speed ICs for photonic networks

4.1 Overview of very-high-speed ICs

40-Gbit/s InP IC technology is one of the keys in constructing photonic networks. In early studies on 40-Gbit/s optical communication systems, we developed basic 40-Gbit/s ICs [13] and applied them to prototype ultrahigh-speed optical transmission systems [14],[15].

We also developed production-level over-40-Gbit/s InP HFET (heterostructure field effect transistor) IC design technology and compact packaging technology to accelerate the further scaling down of systems. The operating speed of the ICs we developed using these technologies was as high as 50 Gbit/s. Their output voltage swing was $0.9 V_{pp}$, which was about twice that in conventional ICs, and large enough to construct commercial 40-Gbit/s optical communication systems. Furthermore, the new surface mount technology we developed using compact leadless chip carrier (LCC) packages and resin printed circuit boards (PCBs) has made it possible to mount these over-40-Gbit/s ICs on commercial system boards.

4.2 Over-40-Gbit/s IC design technology

Figure 10 shows a schematic diagram of a 40-Gbit/s optical transmission system, where each block corresponds to electrical and optical devices. Wideband operation is necessary for these ICs for error-free

transmission. Since the system in Fig. 10 is for long-haul transmission, fiber amplifiers were used. However, for very short reach (VSR) applications, it is important to design receivers with sufficient sensitivity without the use of fiber amplifiers to reduce costs.

We fabricated over-40-Gbit/s ICs using production-level $0.1\text{-}\mu\text{m}$ -gate InP HFET technology [16]. Typical values for the cutoff frequency f_T and transconductance g_m of the FETs were about 200 GHz and 1S/mm , respectively. Multiplexers (MUXes) and demultiplexers (DEMUXes) are key ICs in very-high-speed optical transmission systems, whereas the clock timing design is an important factor. Figure 11 shows a block diagram of a 4:1 MUX IC with (a) the new multi-phase clock architecture we developed [17] and (b) a conventional tree-type architecture. The new architecture using a series-gated 4:1 selector operated with a four-phase clock made it possible to reduce the number of transistors to $1/2$. Since the highest-frequency clock is distributed to only one element in the multi-phase clock architecture, whereas it is distributed to four in the conventional tree-type architecture, the new architecture simplifies the timing design. The power dissipation in the multi-phase clock type MUX is reduced to 1.7 W, which is less than $1/3$ that of the conventional tree type. We also applied a multi-phase clock architecture to DEMUX ICs and succeeded in reducing their power dissipation to 1.4 W.

We confirmed error-free operation for the $2^{31}-1$ PRBS (pseudo-random bit sequence) data input of

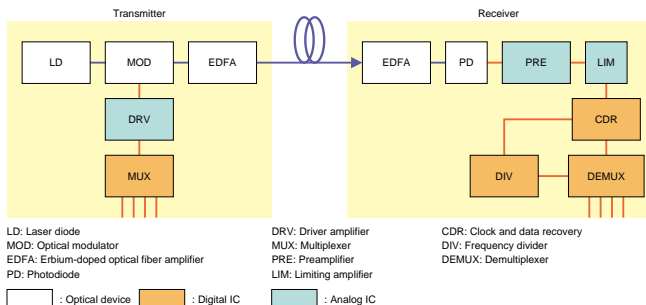


Fig. 10. Schematic diagram of 40-Gbit/s optical transmission systems.

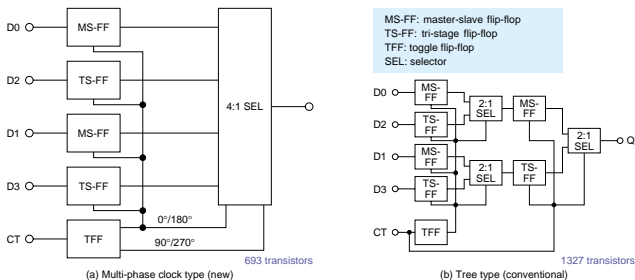


Fig. 11. Block diagram of 4:1 multiplexer IC.

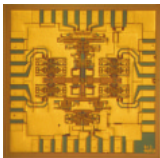


Fig. 12. Photograph of multi-phase clock 4:1 multiplexer IC (2 × 2 mm).

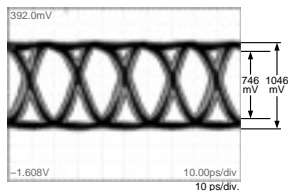


Fig. 13. 50-Gbit/s operating waveform of multi-phase clock 4:1 multiplexer IC.

the 2-mm-square multi-phase clock 4:1 MUX IC (Fig. 12). Its waveform is shown in Fig. 13. The eye height for the multi-phase clock type InP HFET MUX was as large as 746 mV at 50 Gbit/s, which is almost the same as that for a conventional tree type, whereas that for an SiGe HBT MUX is typically 400 mV_{pp}. This means that we achieved a drastic reduction in MUX power dissipation while maintaining a large output voltage swing at 50 Gbit/s.

We also developed a fully monolithic integrated 43-Gbit/s clock data recovery circuit (CDR) [18] (Fig. 14), which enabled us to reduce the number of components mounted in optical transmission systems, which accelerated the miniaturization of systems. The CDR circuit was based on an analog phase locked loop including a voltage-controlled oscillator and it operated with the data-rate clock signal. Error-free operation was confirmed for the 2³¹-1 PRBS data input of the fabricated IC at 43.0184 Gbit/s, which is the data rate of optical channel transport

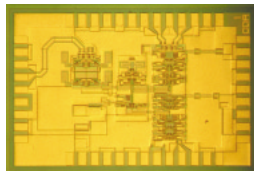


Fig. 14. Clock and data recovery IC (2 × 3 mm).

unit3 (OTU-3), as we can see in Fig. 15.

We also developed a data limiting amplifier with an input sensitivity of 27 mV_{pp} [19]. Capacitive-feedback and inductor peaking techniques widened the bandwidth of the amplifier.

The characteristics of the developed InP HFET ICs

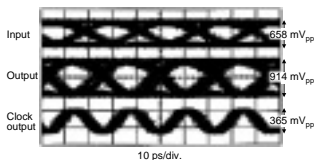


Fig. 15. 43-Gbit/s operating waveforms of CDR IC.

Table 2. Characteristics of developed InP HFET ICs.

Circuit	Operating speed	Power (W)
Clock and data recovery	43 Gbit/s	2.8
4:1 multiplexer	7-50 Gbit/s	1.7
1:4 demultiplexer	4-50 Gbit/s	1.4
Preamplifier	0-40 GHz	0.34
Limiting amplifier	0-50 GHz	0.54

are summarized in Table 2. They reveal a sufficiently high operating speed with reduced power dissipation for 40-Gbit/s-class optical communication systems.

4.3 Packaging technology

Small, wideband packaging technology for over-40-Gbit/s ICs is very important in constructing 40 Gbit/s optical communication systems. We developed an 8-mm-square AlN LCC package and a four-layer resin PCB [20], as shown in Fig. 16. The volume of the LCC package was about 0.14 cm^3 , which is about 1/30 that of a conventional metal package. Based on the results of electromagnetic analysis, grounded vias were arranged around the signal vias to obtain a $50\text{-}\Omega$ matched quasi-coaxial structure. The measured S-parameter data indicated that the 3-dB bandwidth for the package is 60 GHz.

Figure 17 shows a 43-Gbit/s CDR-DEMUX module, which consists of a CDR, a 1:4 DEMUX, and a toggle flip-flop (T-FF) InP HFET LCC-packaged ICs mounted on the resin PCB. We confirmed error-free operation for the $2^{31}-1$ PRBS data input at 43 Gbit/s. This suggests that the volume of the optical receiver module for 40-Gbit/s-class optical communication systems can be reduced to 1/6–1/3 that of conventional prototype modules.

Since LCC packages and resin PCBs have advantages in terms of size, bandwidth, and cost, this packaging technology shows promise for small low-cost over-40-Gbit/s IC modules consisting of very high-speed InP ICs and large-scale Si CMOS devices

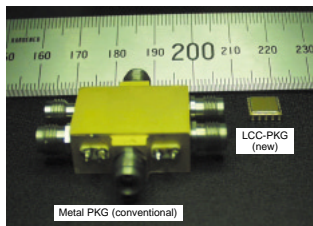


Fig. 16. Developed LCC package (right) and conventional metal package (left).

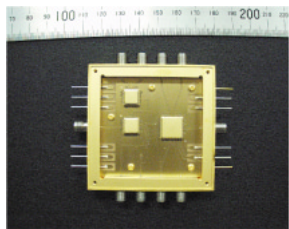


Fig. 17. 43-Gbit/s CDR-DEMUX module.

mounted on the same PCB. The over-40-Gbit/s IC technology and packaging technology should speed up the miniaturization of 40-Gbit/s optical communication systems.

5. Conclusion

We discussed recent progress in the device technologies for optical signal control photonic devices and very high-speed electrical signal processing ICs, which are indispensable in constructing photonic networks.

We discussed wide-range wavelength tunable laser diodes. They will contribute to achieving dynamic signal wavelength switching in photonic networks through which network functions will be drastically increased.

We also discussed PLC switches and AWG multi/demultiplexers, which are the main PLC devices in WDM systems. Further advances in PLC

technologies will contribute greatly to the construction of high-performance photonic networks.

Finally, we discussed the very high-speed signal processing ICs that we have been developing in our laboratories. The over-40-Gbit/s InP HFET ICs developed will accelerate the miniaturization of systems. We will continue to study very high-speed IC technologies especially for 100-Gbit/s systems.

References

- H. Oohashi, Y. Shibata, H. Ishii, Y. Kawaguchi, Y. Kondo, Y. Yoshikuni, and Y. Tohmori, "46.9-nm Wavelength-Selectable Arrayed DFB Lasers with Integrated MMI Coupler and SOA," *IPRM'01*, Nara, Japan, Feb. 1, pp. 575-578, May 2001.
- Y. Yoshikuni, K. Oe, G. Mototsugu, and T. Matsuoaka, "Broad wavelength tuning under distributed feedback lasers," *Electron. Lett.*, Vol. 22, No. 22, pp. 1153-1154, 1986.
- Y. Tohmori, K. Komori, S. Arai, Y. Suematsu, and H. Oohashi, "Wavelength tunable 1.5 μ m GaInAsP/InP bundle-integrated-guide distributed Bragg reflector (BIG-DBR) lasers," *Trans. IEICE*, Vol. E68, pp. 788-790, 1985.
- S. Murata, I. Mito, and K. Kobayashi, "Over 720GHz (5.8nm) frequency tuning by a 1.5 μ m DBR laser with phase and Bragg wavelength control regions," *Electron. Lett.*, Vol. 23, No. 8, pp. 403-405, 1987.
- Y. Tohmori, Y. Yoshikuni, H. Ishii, F. Kano, T. Tamamura, Y. Kondo, and M. Yamamoto, "Broad-range wavelength-tunable Superstructure Grating (SSG) DBR lasers," *IEEE J. Quantum Electron.*, Vol. 29, No. 6, pp. 1817-1823, 1993.
- M. Kawachi, "Recent progress in silica-based planar lightwave circuits on silicon," *IEE Proc. Optoelectron.*, Vol. 143, No. 5, pp. 257-262, Oct. 1996.
- Y. Hibino, T. Maruno, and K. Okamoto, "Recent progress on large-scale PLC technologies with advanced functions," *NTT Review*, Vol. 13, No. 5, pp. 4-9, 2001.
- M. Okuno, T. Goh, S. Sohma, and T. Shibata, "Recent advances in optical switches using silica-based PLC technology," *NTT Technical Review*, Vol. 1, No. 7, pp. 20-30, 2003.
- S. Sohma, T. Goh, H. Okazaki, M. Okuno, and A. Sugita, "Low switching power silica-based super high delta thermo-optic switch with heat insulating grooves," *Electron. Lett.*, Vol. 38, No. 3, pp. 127-128, 2002.
- Y. Hida, Y. Inoue, M. Itoh, M. Ishii, and Y. Hibino, "Development of high-density integrated PLC technologies and their application to AWGs," *NTT Review*, Vol. 13, No. 5, pp. 10-17, 2001.
- Y. Inoue, A. Kaneko, F. Hanawa, H. Takahashi, K. Hattori, and S. Sumida, "Athermal silica-based arrayed-waveguide grating (AWG) multiplexer," *IOOC-ECOC'97*, Edinburgh, U.K., Vol. 5, PD, pp. 33-36, Sep. 1997.
- K. Kato, A. Okada, Y. Sakai, K. Noguchi, T. Sakamoto, S. Suzuki, A. Takahara, S. Kamei, A. Kaneko, and M. Matsuoaka, "32 \times 32 full-mesh (1024 path) wavelength-routing WDM network based on uniform-loss cyclic-frequency arrayed-waveguide grating," *Electron. Lett.*, Vol. 36, No. 15, pp. 1294-1296, July, 2000.
- E. Sano, "Ultra-high-speed Integrated Circuit Technology," *NTT R&D*, Vol. 48, No. 1, pp. 67-72, 1999 (in Japanese).
- H. Toba, Y. Miyamoto, M. Yoneyama, S. Kawashishi, and Y. Yamabayashi, "Next generation ultra-high-speed transmission technologies," *NTT R&D*, Vol. 48, No. 1, pp. 33-42, 1999 (in Japanese).
- K. Hagimoto, M. Yoneyama, A. Sano, A. Hirano, T. Kataoka, T. Otsuji, K. Sato, and K. Noguchi, "Limitations and challenges of single-carrier full 40-Gbit/s repeater system based on optical equalization and new circuit design," *OFEC'97*, Dallas, U.S.A., pp. 242-243, Feb. 1997.
- T. Enoki, H. Yokoyama, Y. Umeda, and T. Otsuji, "Ultra-high-Speed Integrated Circuits Using InP-Based HEMTs," *Jpn. J. Appl. Phys.*, Vol. 37, Part 1, No. 3B, pp. 1359-1364, 1998.
- K. Sano, K. Murata, S. Sugitani, H. Sugahara, and T. Enoki, "1.7-50-Gbit/s InP HEMT 4:1 Multiplexer IC with a Multi-phase Clock Architecture," 2002 IEEE GaAs IC Symp., Monterey, U.S.A., pp. 159-162, Oct. 2002.
- K. Murata, K. Sano, E. Sano, S. Sugitani, and T. Enoki, "Fully monolithic integrated 43 Gbit/s clock and data recovery circuit in InP HEMT technology," *Electron. Lett.*, Vol. 37, No. 20, pp. 1235-1237, 2001.
- K. Sano, K. Murata, S. Sugitani, H. Sugahara, and T. Enoki, "Data Limiting-Amplifier, Data Distributor, and Clock Distributor ICs for 40-Gbit/s-class Optical Communication Systems Using InP HEMTs," 2002 International Conference on Solid State Devices and Materials, Nagoya, Japan, pp. 296-297, Sep. 2002.
- H. Sugahara, S. Kimura, K. Murata, and E. Sano, "Over-40-Gb/s IC Module Technology Using 8-mm-square Leadless Chip Carrier Packages Mounted on Four-Layer Resin Circuit Boards," 2001 IEEE GaAs IC Symp., Baltimore, U.S.A., pp. 255-258, Oct. 2001.



Hiroshi Yasaka

Senior Research Engineer, Supervisor, NTT Photonics Laboratories.

He received the B.S. and M.S. degrees in physics from Kyushu University, Fukuoka in 1983 and 1985, respectively, and the Ph.D. degree in electronic engineering from Hokkaido University, Hokkaido in 1993. In 1985 he joined the Atsugi Electrical Communications Laboratories, NTT. Since then, he has been engaged in R&D on semiconductor photonic devices for optical fiber communication systems. From 1996 to 1998 he joined NTT Optical Network Systems Laboratories, where he has been engaged in R&D on photonic transport systems. Now he is engaged in R&D on semiconductor photonic devices and their monolithically integrated devices. He is a member of the Institute of Electronics, Information and Communication Engineers (IEICE) of Japan, the Japan Society of Applied Physics, the Physical Society of Japan, and IEEE/LEOS.



Masayuki Okuno

Senior Research Engineer, Supervisor, NTT Photonics Laboratories.

He received the B.S., M.S., and Ph.D. degrees in electronic engineering from Hokkaido University, Hokkaido in 1982, 1984, and 2000, respectively. In 1984, he joined NTT Electrical Communications Laboratories, Tokyo, Japan, where he has been engaged in research on optical components and guided-wave optical devices. He is now with NTT Photonics Laboratories, Kanagawa, Japan. He is a member of the IEEE and IEICE.



Hirohiko Sugahara

Senior Research Engineer, Supervisor, NTT Photonics Laboratories.

He received the B.E., M.E., and Dr. Eng. degrees in electrical engineering from Waseda University, Tokyo in 1980, 1982, and 1998, respectively. From 1982, he worked for NTT Laboratories, where he was engaged in the research on the metal-semiconductor contacts and the GaAs IC reliability. He is currently engaged in the development of the InP ICs and subsystems for high-speed optical communications.